Population structure and growth of the broadnose sevengill shark *(Notorynchus cepedianus)* in the Southwestern Atlantic.



Jesus C. Compaire, Gastón A. Trobbiani, Federico Mas, Juan Martín Cuevas, Carolina Pantano, Martín Laporta, Lucas Albornoz, Cristian Lagger, Alejo J. Irigoyen

Fisheries Research 303 (2026) 107896



Contents lists available at ScienceDirect

Fisheries Research

journal homepage: www.elsevier.com/locate/fishres

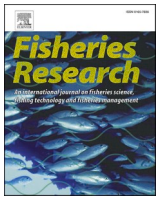

Full length article

Wild population size structure and female-specific growth of the broadnose sevengill shark, *Notorynchus cepedianus*, in the Southwestern Atlantic

Jesus C. Compaire [a,b,*], Gastón A. Trobbiani [a], Federico Mas [c], Juan Martín Cuevas [d], Carolina Pantano [e], Martín Laporta [f,g], Lucas Albornoz [d], Cristian Lagger [e,h,i], Alejo J. Irigoyen [a]

[a] Centro para el Estudio de Sistemas Marinos (CESIMAR), CCT CONICET-CENPAT, Puerto Madryn, Chubut, Argentina
[b] Universidad Nacional de la Patagonia San Juan Bosco (UNPSJB), Facultad de Ciencias Naturales y Ciencias de la Salud, Puerto Madryn, Chubut, Argentina
[c] Laboratorio de Recursos Pelágicos (DINARA-MGAP), Montevideo, Uruguay
[d] Wildlife Conservation Society de Argentina, Buenos Aires, Argentina
[e] Fundación Por el Mar, Buenos Aires, Argentina
[f] Unidad de Gestión Pesquera Atlántica (DINARA-MGAP), La Paloma, Rocha, Uruguay
[g] Universidad de Santiago de Compostela, Campus Do Mar - Campus Internacional de Excelencia, Spain
[h] Instituto de Diversidad y Ecología Animal (IDEA), Consejo Nacional de Investigaciones Científicas y Técnicas (CONICET), Córdoba, Argentina
[i] Universidad Nacional de Córdoba (UNC), Facultad de Ciencias Exactas, Físicas y Naturales (FCEFyN), Córdoba, Argentina

ARTICLE INFO

Keywords:
Hexanchidae
Von Bertalanffy model
Gompertz model
Logistic model
Tag-recapture
Ontogenetic migration
Patagonia

ABSTRACT

Large sharks are globally distributed predators that contribute to the stability and functioning of marine ecosystems. Accurate estimates of their population size structure and growth dynamics are essential for effective conservation and management in the face of ongoing unsustainable fishing pressure. This is particularly critical for the broadnose sevengill shark (*Notorynchus cepedianus*) on the Southwestern Atlantic continental shelf, where this highly mobile species has experienced significant population declines. Its wide-ranging movements, combined with the broad extent of the continental shelf in the region, pose challenges for accurately characterizing its demography. In this context, long-term monitoring studies emerge as a powerful approach for generating critical biological information on the size-structure and growth of demersal migratory species such as *N. cepedianus*, thereby supporting robust population assessments and evidence-based management recommendations. To this end, we integrated over 15 years of tag–recapture data collected in coastal waters of the Southwestern Atlantic (~34.6ºS to ~49.4ºS), including records of sex and total length, and applied three non-linear growth models to estimate female growth dynamics. The results revealed distinct regional variations in size structure across the latitudinal range. Large specimens were most frequently recorded in the central region (41.2ºS – 44.0ºS), whereas the smallest individuals were predominantly captured in the north (≤ 41.2ºS). Model-based age–growth curve reconstructions suggest that females begin the migratory phase at roughly 2–7 years of age and attain maturity at about 8–15 years. These findings underscore the potential of long-term tagging programs to support effective management and regional conservation strategies and actions.

1. Introduction

The broadnose sevengill shark, *Notorynchus cepedianus*, is a large predator distributed across continental and insular shelves - including bays, estuaries, and nearshore waters in tropical and temperate seas - (Compagno, 1984; Compagno, Ebert, and Smale, 1989; Last and Stevens, 1994). Understanding its population size structure and growth patterns is essential for assessing ecosystem health and informing conservation strategies at both regional and global scales. This need is particularly pressing because long-term growth data for *N. cepedianus* in the Southwestern Atlantic (SWA) are currently unavailable, limiting demographic inference, fisheries assessment and conservation planning for a species that has already experienced substantial population declines documented at both scales (Barbini, Lucifora, and Figueroa, 2015; Irigoyen and Trobbiani, 2016; Finucci et al., 2020). These reductions mirror the widespread declines observed across numerous

* Corresponding author at: Centro para el Estudio de Sistemas Marinos (CESIMAR), CCT CONICET-CENPAT, Puerto Madryn, Chubut, Argentina.
E-mail address: jesus.canocompaire@uca.es (J.C. Compaire).

https://doi.org/10.1016/j.fishres.2026.107896
Received 10 March 2026; Received in revised form 28 September 2026; Accepted 7 October 2026
Available online 17 October 2026
0165-7836/© 2026 Elsevier B.V. All rights are reserved, including those for text and data mining, AI training, and similar technologies.

chondrichthyan taxa (Dulvy et al., 2024).

In the SWA, its range extends from 25° to 52°S (Sadowsky, 1969; Guzmán and Campodónico, 1976), with its main distribution along the Uruguayan and Argentine coasts (33 – 50°S). *Notorynchus cepedianus* is considered particularly relevant within the SWA ecosystem (De Wysiecki et al., 2020), alongside the killer whale (*Orcinus orca*), it is one of the few apex predators in the region (Funes et al., 2024; Riverón et al., 2025). A theoretical migration model for the species has described two principal displacement patterns in the SWA. The northward movement involves individuals migrating from Patagonian waters (40° – 47°S) to the Rio de la Plata (33° – 37°S) in autumn, whereas the southward movement represents a return migration along coastal waters, reaching southern latitudes in the summer (De Wysiecki et al., 2020). Additionally, several studies conducted at discrete coastal aggregation sites have documented seasonal patterns of occurrence (Cedrola et al., 2009; De Wysiecki et al., 2018; Irigoyen et al., 2019), and neonates are frequently recorded during late spring and summer in northern areas (36.5° – 40°S; Lucifora, Menni, and Escalante, 2005; Silveira et al., 2018; Jaureguizar et al., 2022, 2023).

Population size structure and growth estimates represent two critical parameters for conservation management. Size structure is typically characterized using length-frequency distributions (Coelho et al., 2017; Compaire et al., 2024), whereas somatic growth is commonly estimated from length-at-age data or tag–recapture data (Erzini, 1994; Petetta et al., 2025). In the case of large, highly mobile species like sharks, implementing these approaches is inherently challenging. Their ability to move across vast distances, coupled with sporadic captures in seasonal or multi-species fisheries, often results in fragmented data that complicates population assessment. Although age and growth studies based on vertebrae have long been used in chondrichthyan ecology (Cailliet, 1990; Goldman et al., 2012; Harry, 2018; Harry et al., 2022), this methodology is subject to several logistical and practical limitations that can compromise age estimates and their interpretation (Harry, 2018, Harry et al., 2022). Direct validation of band-pair deposition periodicity is challenging and is often limited up to a certain age (Wells et al., 2013). In addition, band deposition patterns can vary along the vertebral column and may not be consistently related to age (Natanson et al., 2018). Band counts also become increasingly difficult—and in some cases virtually impossible—to interpret in the outer margins of vertebrae from large adults, potentially leading to substantial underestimation of age (Francis et al., 2007; Passerotti et al., 2014). In *N. cepedianus*, as in other Hexanchiforms, the relatively low degree of vertebral calcification further complicates age estimation using traditional vertebral band counts (Cailliet, 1990; McFarlane et al., 2002). Consequently, alternative methods, including tag–recapture studies, are becoming increasingly important for improving our understanding of age and growth in the broadnose sevengill shark (Engelbrecht et al., 2020). While initial growth rates have been documented for young-of-the-year (YOY) in localized northern areas (Jaureguizar et al., 2022), long-term empirical growth estimates, reconstructed age-at-length trajectories for older individuals, and population-wide size structure analyses remain unavailable across the SWA.

To address these methodological constraints and the lack of biological information across broad spatial and temporal scales, long-term tag-recapture field studies have emerged as a successful technique to study growth and movements of mobile marine predators, as they integrate efforts from scientists, recreational fishers, and the fishing industry (Simpfendorfer, 2000; Pilling, Cotter, and Metcalfe, 2007; Harry, 2018). This study aims to fill this knowledge gap by providing novel insights into the population size structure and female-specific growth dynamics of *N. cepedianus* in the SWA using data from wild populations. Integrating over 15 years of data from two tagging programs, this work provides essential life-history information for the fisheries management—serving as critical inputs for stock assessment models, ecological risk assessments, and productivity estimations— and enables the estimation of the generation length, which constitutes fundamental baseline information for conservation status assessments (Mace et al., 2008).

2. Material and methods

2.1. Study site and data collection

Sampling was conducted in coastal waters of the SWA (34.6°S to 49.4°S) between January 2011 and January 2026, under two main tagging programs. The first program has been conducted since 2011 by the Fish Ecology Laboratory of CESIMAR as part of a series of studies carried out in Golfo Nuevo (~42.7°S; Irigoyen et al., 2015), Caleta Valdés (~42.4°S; Irigoyen et al., 2018), Caleta Malaspina (~45.1°S; Irigoyen et al., 2019), and most recently in the Puerto Deseado Estuary (~47.8°S). The latter in collaboration with the research and shark conservation project of the NGO Por el Mar (Fig. 1). The fishing effort for tagging was carried out throughout all seasons of the year, with additional fishing trips conducted during periods of peak abundance at each site (Cedrola et al., 2009; Irigoyen et al., 2018, 2019). The second program, *Conservar Tiburones en Argentina*, was launched in 2013, to engage shark anglers in shark conservation. Anglers (n = 265) were trained and engaged in conventional tagging duties, best fishing practices and shark conservation issues, with 126 anglers still active today along > 2500 km of coastline from San Clemente del Tuyú (~36°S) to Península de San Julián (~49°S), covering 41 fishing sites. All captured fish were tagged using external Dart-type tags (models FT-1–94 or PDS; Floy Tag and Hallprint Inc.) and basic biological parameters were recorded, including sex and total length (TL) to the nearest cm. Measurements of TL were taken using a flexible fiberglass tape placed from the tip of the snout to the end of the caudal fin, following the natural curvature of the body during the tagging and release procedure established on both projects (Irigoyen et al., 2018). It is important to note that the data collected herein represent nominal records. Because this citizen science framework relies on voluntary angler reports, no direct measures of fishing effort (e.g., fishing hours, number of hooks, or number of angling trips) were recorded. This lack of standardization prevents the calculation of effort-corrected metrics, meaning that these data were utilized strictly for describing size-frequency distributions and growth parameters rather than deriving high-resolution spatial or temporal abundance trends.

2.2. Length and growth analyses

To evaluate differences among specimens collected across a wide latitudinal range, coastal waters were divided into three latitudinal regions based on biogeographical characteristics and the spatial distribution of sampling sites: north (≤ 41.2°S), central (41.2°S < latitude ≤ 44.0°S) and south (> 44.0°S). The northern and southern regions are placed within the Argentine (temperate-warm) and Magellanic (cold) biogeographic provinces, respectively, while the central region - also defined as the North Patagonian Gulfs ecoregion - represents a transition zone between them. The Argentine Province is strongly influenced by the discharge of the Rio de la Plata and borders the Sub-Brazilian region, which is characterized by a subtropical influence (Balech & Ehrlich, 2008). Additionally, this northern region is notable for the richness and abundance of fishery resources (CTMFM, 2025; Compaire et al., 2026, Marcovecchio et al., 2019). The central region stands out as an area of high marine megafaunal richness and diversity, hosting a high presence of marine mammal and seabird colonies (Balech & Ehrlich, 2008; Foro para la Conservación del Mar Patagónico y Áreas de Influencia, 2008). Finally, the southern section lies within the Subantarctic region and is biogeographically defined as a cold domain (Balech & Ehrlich, 2008).

Differences in TL between sexes and among regions were evaluated using the non-parametric Kruskal–Wallis test, as the data did not meet the assumptions of normality and homoscedasticity. Prior to analysis,

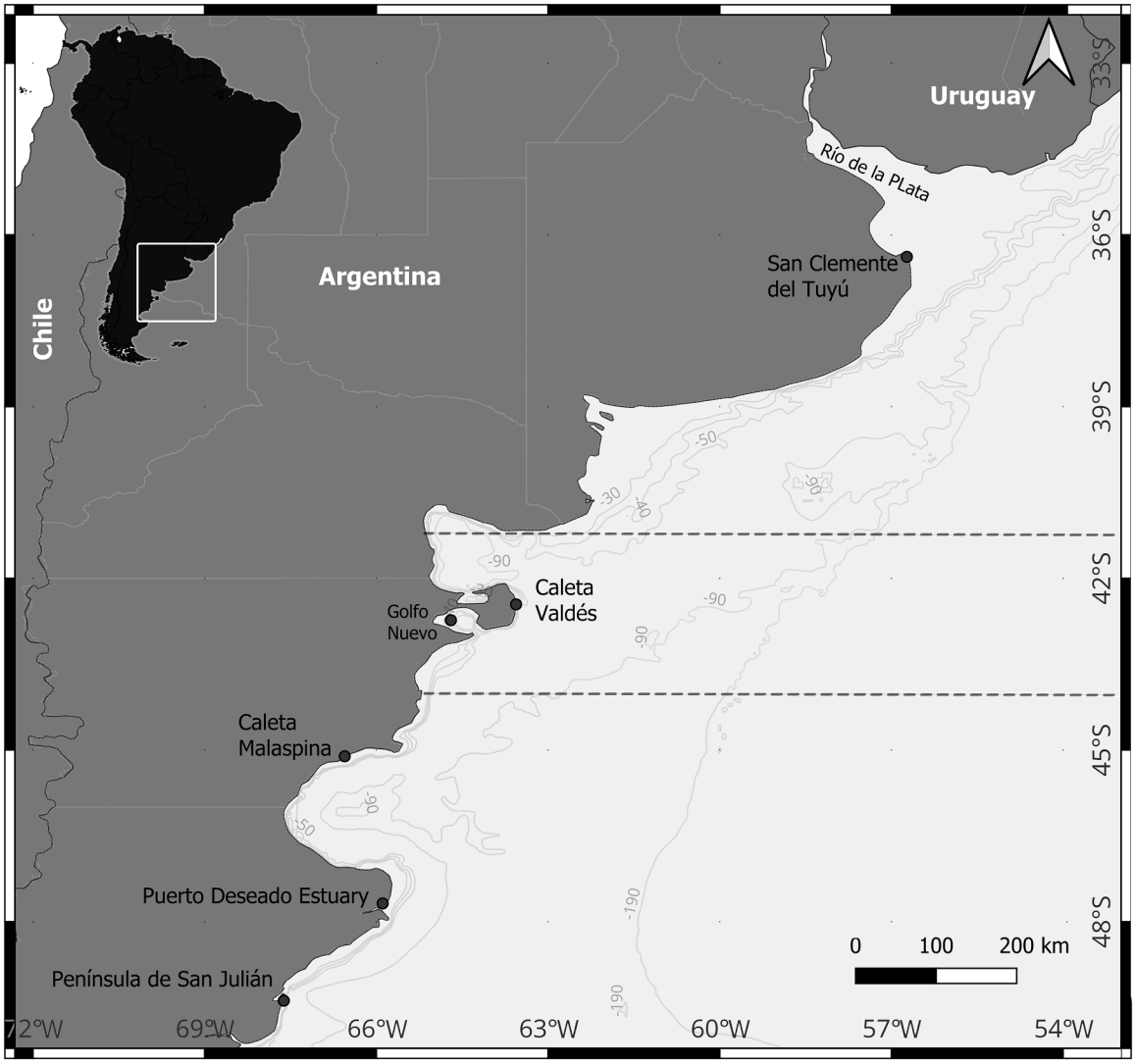

Fig. 1. Study area for *Notorynchus cepedianus* in the southwestern Atlantic Ocean (~34.6°S to ~49.4°S). Latitudinal boundaries among the three regions are delineated by dashed lines: north (≤41.2°S), central (41.2°S < latitude ≤ 44.0°S) and south (latitude > 44.0°S). Bathymetric contours (isobaths) depict the coastal shelf relief.

departures from normality and homoscedasticity were assessed using the Shapiro–Wilk and Levene's tests, respectively. Non-parametric methods were selected because the datasets exhibited significant deviations from parametric assumptions ($p < 0.05$). Post-hoc pairwise comparisons among regions were performed using Dunn's test with Bonferroni correction for multiple comparisons. Kernel density estimation curves were overlaid on histograms to provide a smoothed representation of total length distributions, reducing sensitivity to bin width and facilitating visual comparison among regions. Kernel density curves were estimated using a Gaussian kernel, with a common bandwidth applied across regions for each sex to ensure comparable levels of smoothing. For each sex, the bandwidth was selected using the Improved Sheather–Jones (ISJ) data-driven plug-in method based on observations pooled across regions.

Three non-linear growth models Gompertz (1825), Logistic (Robertson, 1923), von Bertalanffy growth function - VBGF - parameterized following Fabens (1965) were fit to the tag release-recapture data for *N. cepedianus*. Since absolute ages were unknown, we utilized the interval forms of these equations, which relate the length at release (L_1) and recapture (L_2) over a time interval (Δt). Based on empirical size-at-birth and maximum size estimates reported for the study region, the length at birth (L_0) and asymptotic length (L_∞) were fixed at 40 cm (Jaureguizar et al., 2022), and 280 cm (Milessi, 2008), respectively. Fixing L_∞ reduced parameter correlation and improved model stability when fitting tag–recapture growth models. Furthermore, this value aligns closely with the empirical relationship suggested by Taylor (1958) and Pauly (1984), where $L_\infty \approx L_{max} / 0.95$. Applying this rule to our largest recorded specimen (265 cm) yields a theoretical reference of ≈ 279 cm, supporting the choice of 280 cm as a biologically plausible baseline threshold for the regional population. The Francis (1988) parametrization was evaluated but yielded identical likelihoods and growth trajectories to the Fabens formulation under L_∞ fixed, and was therefore not treated as an independent model. In all models, K denotes the growth coefficient. However, it is important to note that despite K representing a rate parameter in all models, its mathematical definition and biological interpretation depend on the functional form. In the VBGF - Fabens (1965), K determines the rate at which length approaches the asymptotic length (Pauly, 1980). In contrast, in sigmoidal models such as the Gompertz (1825) and Logistic (Robertson, 1923), K describes the exponential decay of the relative growth rate, and the resulting growth trajectories are characterized by the presence of an inflection point (Katsanevakis and Maravelias, 2008). The models are described as follows:

Gompertz (1825): A model where the growth rate decreases

exponentially with size, suitable for non-symmetric sigmoidal growth:

$$L_2 = L_\infty \cdot e^{\ln\left(\frac{L_1}{L_\infty}\right)e^{-K\Delta t}}$$

Fabens (1965): A non-linear method that fits data directly to the VBGF by minimizing the residuals between observed and predicted recapture lengths:

$$L_2 = L_\infty - (L_\infty - L_1)e^{-K\Delta t}$$

Logistic (Robertson, 1923): Describes a sigmoidal growth curve symmetric around its inflection point:

$$L_2 = \frac{L_\infty}{1 + \left(\frac{L_\infty}{L_1} - 1\right)e^{-K\Delta t}}$$

Data for the growth analysis was restricted to individuals with reliable total length measurements at both release and recapture. To ensure the integrity of the dataset and minimize the influence of potential measurement errors, the analyses were performed on specimens exhibiting annual growth rates up to 40 cm yr^{-1} (Van Dykhuizen and Mollet, 1992). This threshold represents the upper limit of the growth rate calculated for 1-year-old individuals of this species, which enter the baseline study at sizes $\leq$ 120 cm TL (Van Dykhuizen and Mollet, 1992). Following this quality filtering, for specimens recaptured more than once (up to two recapture events), each tag–recapture interval was treated as an independent observation, provided that reliable length measurements were recorded at both the beginning and end of the interval. Since growth rates inherently decrease with size and our dataset consists exclusively of larger specimens ($\geq$ 133 cm TL), allowing annual increments higher than this theoretical ceiling for small, fast-growing sharks would incorporate obvious field measurement errors. Additionally, two sensitivity analyses were conducted by refitting the growth models: first, including zero-growth records to evaluate the impact of filtering non-positive increments, and second, using a subset restricted to individuals with a time at liberty of at least 60 days to assess potential bias from short-term recaptures (Simpfendorfer, 2000). Because growth rates in elasmobranchs can be sex-dependent (Braccini et al., 2010; Liu et al., 2021; Simpfendorfer, 2000), we evaluated the relationship between length increment and time at liberty for males and females separately prior to model fitting. Residual diagnostics were conducted for the non-linear models fitted by maximum likelihood assuming homoscedastic Gaussian errors on recapture length. These diagnostics included tests for normality (Shapiro–Wilk), length-dependent residual structure (Spearman rank correlation between residuals and initial length), and non-random residual structure (Wald–Wolfowitz runs test). The performance among models was evaluated using the bias-corrected Akaike's Information Criterion (AICc) (Burnham, Anderson, 2002). Because the absolute value of the AICc by itself is not informative, we computed the differences in AICc from the minimum AICc value to assess relative model performance as $\Delta AICc = AICc_i$ - AICcmin. The $\Delta AICc$ values allow for a quick comparison and ranking of candidate models. Models with $\Delta AICc < 2$ have statistical support (Burnham, Anderson, 2002). For all candidate non-linear models fitted by maximum likelihood, the total number of estimated parameters was set to 2, which accounts for the single structural growth parameter estimated (K, given that L_∞ was fixed) plus the residual variance (σ^2) treated as an additional estimated parameter in the likelihood function. To illustrate growth patterns, age-length trajectories were reconstructed by anchoring the models at birth size.

2.3. Data processing and software

Statistical analyses were performed using Python (version 3.12.2; Python Software Foundation, https://www.python.org). Non-parametric comparisons of TL were conducted using the SciPy library v1.16.1; Virtanen et al., (2020)). When significant differences were detected, post hoc pairwise comparisons were performed using Dunn's test as implemented in the scikit-posthocs package v0.11.4; Terpilowski, (2019)). Additional statistical diagnostics and data exploration were supported by Statsmodels v0.14.5; Seabold and Perktold, (2010)).

3. Results

Out of 1133 *N. cepedianus* specimens identified, TL was recorded for 1109 (sex was unrecorded for 12 individuals). Specimens ranged from 45 to 265 cm ($\bar{x} \pm SD = 180.5 \pm 44.1$ cm; Fig. 2), with females being significantly larger than males (185.1 ± 46.5 cm vs. 169.8 ± 33.8 cm; KW test: $H(1) = 42.81$, $p < 0.001$; median [interquartile range, IQR] = 192 [154.8 – 222] cm vs. 177 [148 – 196] cm, respectively). Significant regional differences were also observed ($H(2) = 414.47$, $p < 0.001$); specimens from the central region (208.56 ± 27.65, 210 [191 – 230] cm, n = 511) were larger than those from both the southern (166.23 ± 27.51, 164.5 [145 – 182] cm, n = 254; Dunn test, $Z = 14.41$, adjusted $p < 0.001$) and northern (149.45 ± 47.81, 145 [114 –187] cm, n = 344; Dunn test, $Z = 18.65$, adjusted $p < 0.001$). Conversely, no significant difference in total length was detected between the southern and northern regional samples (Dunn test, $Z = 2.35$, adjusted $p > 0.057$). Intra-regional analyses revealed that females were significantly larger than males in the central (KW test: $H(1) = 106.97$, $p < 0.001$) and southern (KW test: $H(1) = 9.30$, $p = 0.002$) regions, whereas no significant difference between sexes was detected in the northern region (KW test: $H(1) = 1.63$, $p = 0.202$). A detailed summary of abundance, and length statistics by region and sex is provided in Table 1, while their respective length frequency distributions are illustrated in Fig. 2.

From 71 tag–recaptured events, 50 recaptures remained after applying annual growth-rate filtering criteria (Table 2). The remaining 21 recaptures were excluded due to negative or zero growth rates resulting from potential measurement errors (n = 15), or implausibly high growth rates exceeding 40 cm yr^{-1} (n = 6). The final dataset included three specimens that were recaptured twice, with each of their distinct recapture intervals retained as an independent observation. A significant positive relationship between length increment and time at liberty was detected only in females (Pearson's r = 0.674, 95% CI = 0.448, 0.819, $p < 0.001$, n = 37), whereas no such relationship was observed in males (Pearson's r = -0.238, 95% CI = −0.698, 0.360, $p = 0.433$, n = 13), likely constrained by the small sample size and limited statistical power. Consequently, growth model fitting and comparison were conducted exclusively using female specimens. Tag-recapture selected females were at liberty between 12 and 1488 days, and their size ranged from 133 to 261 cm. Although this included short-term recaptures, these records were retained as their annualized growth rates fell within biologically plausible limits. Estimates of the growth coefficients (K) were 0.122, 0.145, and 0.169 yr^{-1} for the Fabens (VBGF), Gompertz, and Logistic models, respectively. Sensitivity analyses refitting models with zero-growth increments (n = 39) and excluding individuals with < 60 days at liberty (n = 30) yielded highly consistent and robust growth parameter estimates. Residual diagnostics indicated that candidate models fitted to both the filtered (n = 37) and the restricted (n = 30) datasets satisfied the assessed statistical assumptions ($p > 0.05$ across all tests). Specifically, the residuals consistently satisfied the assumptions of normality (Shapiro-Wilk, $p > 0.05$), lack of length-dependency (Spearman, $p > 0.05$), and randomness in residual distribution (Runs test, $p > 0.05$). Notably, while incorporating zero-growth records in the expanded dataset (n = 39) preserved near-identical parameter estimates, it introduced a slight departure from residual randomness in the runs test ($p < 0.05$), supporting the retention of n = 37 as the primary analytical framework. Across all the three dataset configurations, the model selection hierarchy remained identical all candidate models received substantial support ($\Delta AICc < 2$), with the Gompertz model consistently exhibiting the highest relative support

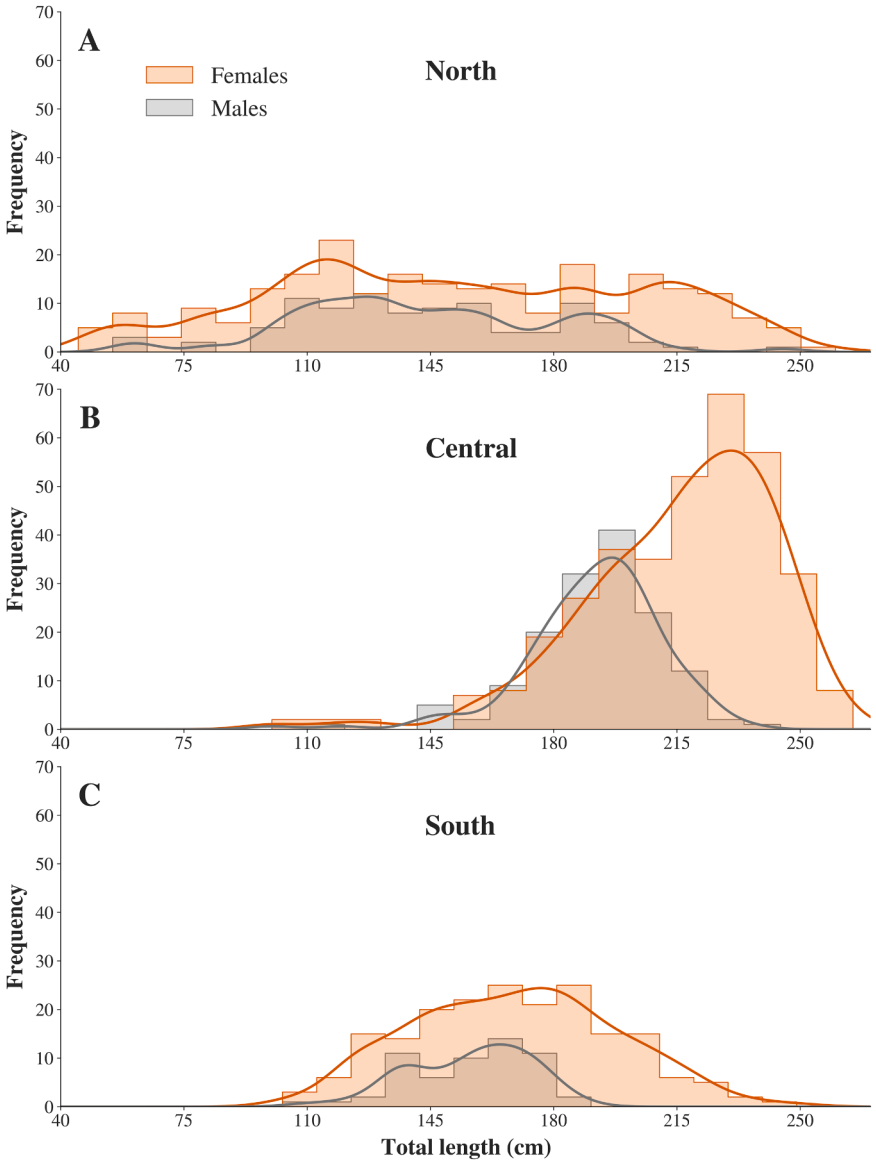

Fig. 2. Length frequency distributions of *Notorynchus cepedianus* total length (TL, cm) disaggregated by sex (females: orange; males: grey) within each geographical region: (A) north (≤ 41.2°S), (B) central (41.2°S < latitude ≤ 44.0°S), and south (> 44.0°S). Histograms are presented with 10 cm bins, and kernel density estimation curves are overlaid to illustrate the smoothed length distributions.

Table 1
Sample size (n), total length (TL) range, mean TL (± SD), and median TL [interquartile range, IQR] of *Notorynchus cepedianus* disaggregated by region and sex in the Southwestern Atlantic (Note that the 12 specimens of unknown sex were not included).

Region	Sex	n	TL range (cm)	TL mean ± SD (cm)	Median [IQR] (cm)
North	Female	240	45 – 260	152.20 ± 51.69	150 [113.5 – 195]
	Male	97	59 – 245	144.06 ± 36.52	140 [118 – 170]
Central	Female	357	100 – 265	216.06 ± 26.87	220 [200 – 236]
	Male	150	100 – 235	191.78 ± 19.33	195 [182.3 – 204]
South	Female	195	103 – 249	168.86 ± 28.98	170 [146 – 188.5]
	Male	58	110 – 188	156.17 ± 17.11	158.5 [140.5 – 170]

(ΔAICc = 0) and nearly identical growth coefficients (K = 0.1450 *vs.* 0.1446 yr^{-1} for the filtered and restricted datasets, respectively Table 3).

The growth curves generated by the Fabens (VBGF), Gompertz, and Logistic models (Fig. 3) illustrated consistent asymptotic behavior toward the fixed value of L_∞, with all three trajectories naturally converging at larger body sizes. It is critical to note that this late-stage convergence is expected and mathematically driven by the fact that L_∞ was fixed during the model-fitting process. However, marked differences in growth trajectories remained during early and intermediate life stages. The Fabens (VBGF) model predicted the fastest early growth, reaching larger sizes at younger ages compared with the other two models. In contrast, the Logistic model exhibited a more gradual increase in length, particularly for small individuals, resulting in smaller predicted sizes at intermediate ages. Finally, the Gompertz model displayed an intermediate pattern, with growth rates lower than those of

Table 2
Tag–recapture records for *Notorynchus cepedianus*, showing total length at recapture (TL recapture), time at liberty (days), observed length increment (ΔTL), annualized growth rate (cm yr^{-1}), and sex for each recaptured individual. Total length at release can be derived directly as TL recapture - ΔTL. TL: total length, F: female, M: male.

Date	Recapture	TL recapture (cm)	Days at liberty	ΔTL (cm)	Growth rate (cm yr^{-1})	Sex
2016–01–12	1	217	59	3	18.559	F
2016–03–12	2	191	119	11	33.739	F
2016–03–12	3	157	60	5	30.417	F
2016–08–07	4	205	267	5	6.835	F
2016–10–05	5	195	326	6	6.718	F
2016–11–05	6	230	357	5	5.112	F
2016–12–03	7	192	385	14	13.273	F
2016–12–03	8	181	59	5	30.932	F
2016–12–03	9	207	385	4	3.792	M
2017–01–30	10	238	58	6	37.759	F
2017–11–09	11	246	369	17	16.816	F
2017–11–10	12	250	370	8	7.892	F
2017–11–10	13	199	284	7	8.996	F
2017–11–12	1	235	670	18	9.806	F
2018–03–18	14	187	59	1	6.186	F
2018–11–10	15	240	766	12	5.718	F
2019–01–21	16	172	131	3	8.359	F
2019–01–21	17	170	368	6	5.951	F
2019–01–21	18	210	368	12	11.902	F
2019–10–30	19	224	1120	29	9.451	F
2019–11–16	20	197	1106	5	1.650	M
2019–11–16	21	205	1106	7	2.310	M
2019–11–16	22	241	1078	27	9.142	F
2019–11–16	8	213	1078	37	12.528	F
2019–11–17	23	184	372	8	7.849	M
2019–11–17	24	204	372	11	10.793	M
2019–11–27	25	235	1089	18	6.033	F
2019–11–28	26	261	12	1	30.417	F
2019–12–18	27	202	32	2	22.812	M
2019–12–18	28	224	403	8	7.246	F
2019–12–19	29	241	769	4	1.899	F
2019–12–19	30	231	51	1	7.157	F
2019–12–19	9	210	1111	7	2.300	M
2020–11–15	31	191	333	9	9.865	M
2020–11–15	32	201	365	12	12.000	M
2020–11–15	33	185	736	7	3.471	M
2020–11–15	34	204	1099	3	0.996	M
2020–11–15	35	213	389	3	2.815	M
2020–11–15	36	232	389	5	4.692	F
2020–12–02	37	222	349	6	6.275	F
2020–12–02	38	218	371	1	0.984	F
2020–12–02	39	242	1488	7	1.717	F
2024–09–15	40	172	169	3	6.479	F
2025–08–12	41	133	313	7	8.163	F
2025–10–01	42	210	385	12	11.377	F
2025–10–11	43	187	250	14	20.440	F
2025–10–23	44	191	1104	1	0.331	M
2026–01–16	45	181	360	10	10.139	F
2026–01–17	46	202	351	8	8.319	F
2026–01–17	47	142	40	1	9.125	F

the Fabens (VBGF) model at early ages but higher than the Logistic model. Since our observed size range was bounded between 133 and 261 cm TL, any reconstructed trajectory outside these limits constitutes a purely theoretical extrapolation based on L_0 and L_∞. Consequently, all age estimations derived from growth curve behaviors outside these bounds are entirely governed by the mathematical structure of each candidate model, warranting caution when making biological interpretations beyond the observed size range.

4. Discussion

This study assessed the population size structure and female-growth rates of *N. cepedianus* in the coastal waters of the SWA using 15 years of tag release-recapture data. Our findings reveal distinct latitudinal variations in size structure; the highest frequency of large specimens was recorded in the central region, followed by those from the southern waters, while the distribution peaked at smaller sizes for individuals captured in the northern region. This spatial pattern in size structure across regions supports previous hypotheses identifying northern Argentina and Uruguay as the species' primary parturition and neonate nursery areas (Silveira et al., 2018; De Wysiecki et al., 2020; Jaureguizar et al., 2023), as highlighted by the presence of smaller individuals (45–100 cm TL) in the northern region. High prey availability and favorable environmental conditions have been identified as the key drivers underlying the use of coastal habitats in this region as nursery areas for the species (Jaureguizar et al., 2023). This spatial segregation introduces a new movement hypothesis for the species, suggesting that around 100 cm TL juveniles undergo an ontogenetic shift, leaving the nursery grounds to enter a migratory phase. The size structure of individuals from the central zone indicates that organisms are significantly larger and, consequently, include a high proportion of adults of both sexes. This demographic distinction is largely driven by data from Caleta Valdés, which is so far the only known aggregation site for both mating and feeding purposes in the SWA (Irigoyen et al., 2018; Funes et al., 2024). Hence, the observed size-structure pattern in the central zone may be biased by the concentration of samples obtained from a reproductive area of the species.

The length range analyzed to assess population size structure and growth rates in the SWA was comparable to that reported in other regions for wild populations (52 – 284 cm in southern Australia: Braccini et al., 2010; 61 – 286 cm in southern Africa: Engelbrecht et al., 2020) and captive specimens, although the latter spanned narrower size spectrums (48 – 240 cm at Melbourne Aquarium: Braccini et al., 2010; 65 – 188 cm at Monterey Bay Aquarium: Van Dykhuizen and Mollet, 1992). To accurately translate the observed length distributions into growth estimates, we employed a multi-model approach as recommended for elasmobranchs (Liu et al., 2021). We compared three non-linear models commonly utilized in shark growth studies: the VBGF via Fabens (1965), Gompertz (1825), and Logistic (Robertson, 1923) models (Van Dykhuizen and Mollet, 1992; Cailliet and Goldman, 2004; Cailliet et al., 2006). All candidate models exhibited adequate fit to the data ($\Delta AICc < 2$), describing rapid early growth followed by progressive deceleration as individuals approach the asymptotic length (L_∞ = 280 cm). Such results indicate a lack of clear support for a single growth function describing the growth trajectory of *N. cepedianus* females in the SWA. The statistical support across models reflects a common limitation of tag–recapture growth studies, in which tagging data contain no unambiguous information on absolute age (Francis, 1988), and therefore potential age-dependent variation in growth cannot be explicitly modelled. In the absence of such information, our data do not allow us to determine whether early growth in *N. cepedianus* females follows the strict trajectory of the VBGF or the sigmoidal patterns predicted by the Gompertz and Logistic models. However, this uncertainty is restricted to smaller sizes, as the model trajectories and confidence intervals converge and broadly overlap once individuals exceed approximately 200 cm TL within the observed range.

The estimated growth coefficient for females in this study derived from tag-recapture data based on the VBGF parametrization following Fabens falls within the range of previous estimates reported for captive females, which ranged from K = 0.122 to 0.235 (Braccini et al., 2010) and reach up to K = 0.29 (Van Dykhuizen and Mollet, 1992). However, this estimate remains higher than those reported for other wild female populations (K = 0.072–0.089: Braccini et al., 2010). To evaluate our findings alongside regional estimates for wild YOY females in the SWA, comparisons were restricted strictly within equivalent model formulations, as growth parameters carry distinct mathematical meanings across different equation families. Across all three tested models, our estimated growth coefficients were substantially lower than those reported for wild YOY females, whose growth coefficients ranged from 0.0689 to 0.3741 for the VBGF, 0.8508–1.5717 for the Gompertz model,

Table 3
Growth parameter estimates and sensitivity analysis for *Notorynchus cepedianus* females. Estimates of the growth coefficient (K) and corresponding 95% confidence intervals (CI), bias-corrected Akaike's Information Criterion differences (ΔAICc) for comparison of candidate non-linear growth models fitted by maximum likelihood estimation, and residual diagnostics are presented across three datasets: filtered dataset (n = 37), an expanded dataset including zero-growth increments (n = 39), and a restricted subset excluding short-term recaptures (≥ 60 days at liberty, n = 30). Residual diagnostics include the Shapiro–Wilk test for normality (W), Spearman rank correlation test for length-dependence (ρ), and the runs test for randomness (Z); reported values are p-values.

Models	Dataset	K (95% CI)	ΔAICc	W	ρ	Z
Fabens (VBGF)	Filtered	0.1220 (0.0996 – 0.1395)	1.0270	0.7979	0.5350	0.0671
	Expanded	0.1219 (0.0971 – 0.1406)	1.1295	0.6349	0.3714	0.0371
	Restricted	0.1217 (0.0967 – 0.1409)	0.8497	0.9059	0.6123	0.5117
Gompertz	Filtered	0.1450 (0.1187 – 0.1652)	0	0.6272	0.9439	0.0710
	Expanded	0.1450 (0.1153 – 0.1659)	0	0.4421	0.8515	0.0413
	Restricted	0.1446 (0.1148 – 0.1656)	0	0.6890	0.8089	0.5873
Logistic	Filtered	0.1688 (0.1354 –0.1934)	1.1900	0.3344	0.6050	0.0710
	Expanded	0.1687 (0.1327 – 0.1943)	1.2235	0.2033	0.7179	0.0413
	Restricted	0.1683 (0.1323 – 0.1937)	1.0303	0.4435	0.3707	0.5873

and 1.6374–2.2823 for the Logistic model (Jaureguizar et al., 2022). While this independent regional study confirms very rapid initial growth in neonates, it cannot validate the early trajectories of our curves since our dataset lacks individuals smaller than 133 cm TL. Applying our reconstructed growth curves, individuals of approximately 100 cm TL that hypothetically begin their migratory phase- or, alternatively, begin to be captured in the central and southern regions analyzed- are estimated to be between 2 and 7 years old in female *N. cepedianus*. However, due to the lack of small individuals in our dataset, this early timeline remains strictly model-dependent. Based on this age-growth reconstruction and the female maturity length previously reported for the SWA (190 cm TL: Irigoyen et al., 2018), females in this region would reach sexual maturity at between 8 and 15 years of age. The total of males tagged and recaptured was insufficient to provide a robust estimation of growth parameters for this sex, as the limited sample size potentially constrained the statistical power required to detect significant growth trends.

The number of males captured was substantially lower than that of females, representing approximately a 1:3 (male:female) ratio. Three non-exclusive speculative explanations may account for this pattern: (1) coastal areas, where fishing effort was concentrated, may be used less frequently by males; (2) males may experience higher mortality; or (3) males may show lower selectivity for the bait or hook-based fishing gear. While empirical data to support these hypotheses are not available, the first explanation – spatial segregation– appears to be the most plausible and could be further evaluated through satellite telemetry by tracking individuals of both sexes.

Our findings provide a novel long-term empirical growth baseline for wild *N. cepedianus* in the SWA, yet some methodological considerations warrant attention. First, as inherent to tag–recapture data, individuals lack absolute age information, requiring growth trajectories to be anchored to a fixed birth length (L_0 = 40 cm), which introduces model-dependent uncertainty in early age-at-size reconstructions. Second, while fixing asymptotic length (L_∞ = 280 cm) was methodologically required to reduce parameter correlation and was biologically justified by empirical relationships (see Methods), holding L_∞ constant conditions the estimation of K to this pre-defined threshold. Third, potential spatial sampling bias exists, as tagging effort was concentrated at specific coastal aggregation sites (e.g., mating grounds in Caleta Valdés and northern nurseries). Finally, the low number of male recaptures

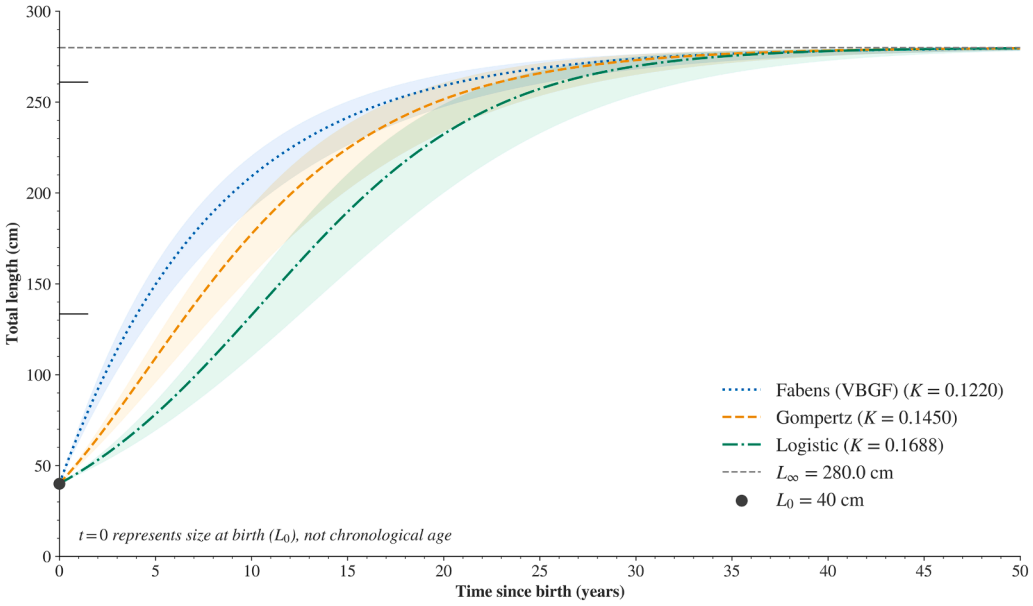

Fig. 3. Growth curves for tag – recaptured *Notorynchus cepedianus* females estimated using three non-linear models: the von Bertalanffy growth function (VBGF) parameterized using the Fabens method (dotted blue line), Gompertz (dashed orange line), and Logistic (dashed-dotted green line). Shaded areas represent the 95% confidence interval for each curve. The length at birth (L_0) is depicted by a black dot ($t = 0$), and the fixed asymptotic length (L_∞) by a grey dashed line. Short horizontal lines along the y-axis indicate the observed range of total lengths (133 – 261 cm) used to estimate growth. Note that growth trajectories outside this empirically observed size range — both the early growth back-extrapolated to L_0 and the asymptotic growth extrapolated beyond 261 cm towards L_∞ — represent mathematical reconstructions based on model assumptions and should be interpreted as theoretical trajectories rather than empirically fitted data.

precluded sex-specific growth modeling, restricting our empirical growth trajectories strictly to females.

Beyond their biological relevance, the empirical population size structure, growth parameters and age-growth reconstructions obtained in this study provide essential inputs for fisheries management and stock assessment tools in the SWA. In data-limited scenarios, these empirical life-history parameters enable the application of length-based stock assessment models (García-García et al., 2026). Furthermore, key parameters such as K and age-at-maturity are directly linked to population vulnerability—particularly in large elasmobranchs ($L_{max} > 200$ cm) where late maturity heavily dictates resilience to exploitation (Frisk et al., 2001). Incorporating these regional baselines into future management frameworks may help reduce uncertainty when designing precautionary conservation measures, evaluating species vulnerability, and establishing spatial monitoring strategies across the SWA.

5. Conclusions

Our study provides novel long-term empirical growth dynamics and model-derived age estimates for female *Notorynchus cepedianus* in the Southwestern Atlantic (SWA), offering critical insights into its ontogenetic distribution. While our findings align with the documented use of northern nursery grounds by younger specimens (Silveira et al., 2018; Jaureguizar et al., 2023), our work incorporates a new movement hypothesis for the species in which older individuals expand into central and southern regions, contextualizing these ontogenetic movements within a temporal framework. Specifically, the presence of free-swimming individuals as small as 45 cm TL in the northern region supports the biological plausibility of the selected birth length ($L_0 =$ 40 cm) reported for this area (Jaureguizar et al., 2023), and is consistent with neonate or YOY size ranges. By applying our age-growth reconstructions to the previously reported migratory size threshold of approximately 100 cm TL, we estimate that females would enter this hypothetic migratory phase and recruit to meridional regions at an age of 2 – 7 years, depending on the growth model used. While these reconstructed timelines remain strictly model-dependent, the lower end of this range (e.g., ~2 years derived from the VBGF) is consistent with the rapid early growth independently reported for regional YOY cohorts (Jaureguizar et al., 2022). Following this potential ontogenetic shift, and based on the maturity length reported for the region (Irigoyen et al., 2018), model projections indicate that females would subsequently reach sexual maturity between 8 and 15 years of age. It is critical to underscore that since tag–recapture data do not provide direct age estimates, these timelines represent theoretical reconstructions anchored at birth size. This approach inherently introduces a degree of uncertainty linked to the mathematical structure of each growth function, highlighting the model-dependent nature of such estimations. Nevertheless, they constitute essential demographic references for population size assessments in scenarios where direct ageing structures are unavailable. Consequently, these projections provide a highly valuable and biologically coherent framework for understanding the growth of *N. cepedianus* females in the region.

Given the high mobility and wide distribution of this species, the findings presented here reinforce the suitability of long-term tagging programs for providing critical biological information on population size structure and growth. Such data are essential for the effective management and regional conservation of *N. cepedianus* in the SWA, as well as for strengthening monitoring frameworks and future population assessments. In particular, the biological parameters estimated in this study provide key inputs for detecting temporal changes in demographic structure and offer a novel baseline for estimating generation length based on wild populations data (Finucci et al., 2020). This information not only strengthens IUCN Red List conservation status assessments, but also provides essential metrics for stock assessment, demographic modeling, and ecological risk assessment, thereby reinforcing long-term monitoring frameworks and adaptive management strategies in the Southwestern Atlantic.

CRediT authorship contribution statement

Jesus C. Compaire: Methodology, Software, Formal analysis, Data curation, Investigation, Visualization, Writing – original draft, Writing – review & editing. **Gastón A. Trobbiani:** Writing – review & editing, Visualization, Resources, Conceptualization. **Federico Mas:** Writing – review & editing, Resources. **Juan Martín Cuevas:** Writing – review & editing, Resources, Conceptualization. **Carolina Pantano:** Writing – review & editing, Resources, Data curation, Conceptualization. **Martín Laporta:** Writing – review & editing, Resources. **Lucas Albornoz:** Writing – review & editing, Resources. **Cristian Lagger:** Writing – review & editing, Resources. **Alejo J. Irigoyen:** Writing – review & editing, Writing – original draft, Supervision, Resources, Methodology, Investigation, Data curation, Conceptualization.

Declaration of Generative AI and AI-assisted technologies in the writing process

During the preparation of this work the author(s) used AI in order to improve readability and language. After using this tool/service, the author(s) reviewed and edited the content as needed and take(s) full responsibility for the content of the publication.

Funding

This study did not receive any specific funding.

Declaration of competing interest

The authors declare that they have no known competing financial interests or personal relationships that could have appeared to influence the work reported in this paper.

Acknowledgments

This study especially acknowledges all the individuals who participated in the citizen science program "*Conservar Tiburones en Argentina*" and in the research activities that made it possible. We are also grateful to the Williams Foundation for the support provided to improve computing capacity through the "*2024 Complementary Funds for Research Projects with Impact on the Argentine Territory*". We are highly grateful to two anonymous reviewers whose constructive comments, thorough insights, and solid expertise significantly strengthened and improved the quality of this manuscript. This research received no specific grant from any funding agency in the public, commercial, or not-for-profit sectors for the payment of Article Processing Charges. Consequently, as the primary research was conducted in a middle-income country with limited resources, the corresponding author has opted for the subscription-based model.

Data availability

Data will be made available on request. Code and analysis workflows used in this study are open access and permanently archived on Zenodo (https://doi.org/10.5281/zenodo.23262986), with ongoing development maintained on GitHub (https://github.com/jcompaire/FishGrowth_Ncepedianus).

References

Balech, E., Ehrlich, M.D., 2008. Esquema biogeográfico del Mar Argentino. Rev. De. Invest. óN. Y. Desarro. Pesq. 19, 45–75.

Barbini, S., Lucifora, L., Figueroa, D., 2015. Using opportunistic records from a recreational fishing magazine to assess population trends of sharks. Can. J. Fish. Aquat. Sci. 72, 1853–1859. https://doi.org/10.1139/cjfas-2015-0087.

Braccini, J., Troynikov, V., Walker, T., Mollet, H., Ebert, D., Barnett, A., Kirby, N., 2010. Incorporating heterogeneity into growth analyses of wild and captive broadnose sevengill sharks *Notorynchus cepedianus*. Aquat. Biol. 9, 131–138. https://doi.org/10.3354/ab00246.

Burnham, K., Anderson, D., 2002. Model Selection and Multimodel Inference. Springer New York, New York, NY. https://doi.org/10.1007/b97636.

Cailliet, G.M., 1990. Elasmobranch age determination and verification: an updated review. NOAA Tech. Rep. NMFS 90, 157–165.

Cailliet, G.M., Smith, W.D., Mollet, H.F., Goldman, K.J., 2006. Age and growth studies of chondrichthyan fishes: the need for consistency in terminology, verification, validation, and growth function fitting. Environ. Biol. Fishes 77, 211–228. https://doi.org/10.1007/s10641-006-9105-5.

Cailliet, G., Goldman, K. (2004). Age Determination and Validation in Chondrichthyan Fishes, in: Biol. Sharks Their Relat. January 2017, pp. 399–447. doi:10.1201/9780203491317.pt3.

Cedrola, P., Caille, G., Chiaramonte, G., Pettovello, A., 2009. Demographic structure of broadnose seven-gill shark, *Notorynchus cepedianus*, caught by anglers in southern Patagonia, Argentina. Mar. Biodivers. Rec. 2, e138. https://doi.org/10.1017/S1755267209990558.

Coelho, R., Mejuto, J., Domingo, A., Yokawa, K., Liu, K.-M., Cortés, E., Romanov, E.V., da Silva, C., Hazin, F., Arocha, F., Mwilima, A.M., Bach, P., Ortiz de Zárate, V., Roche, W., Lino, P.G., García-Cortés, B., Ramos-Cartelle, A.M., Forselledo, R., Mas, F., Ohshimo, S., Courtney, D., Sabarros, P.S., Perez, B., Wogerbauer, C., Tsai, W.-P., Carvalho, F., Santos, M.N., 2017. Distribution patterns and population structure of the blue shark (Prionace glauca) in the Atlantic and Indian Oceans. Fish Fish. 19 (1), 90–106. https://doi.org/10.1111/faf.12238.

Compagno, L. (1984). FAO Species Catalogue. Vol. 4. Sharks of the world. An annotated and illustrated catalogue of shark species known to date. Part 1 - Hexanchiformes to Lamniformes. FAO ed., Rome, Italy.

Compagno, L., Ebert, D., Smale, M., 1989. Guide sharks rays South. Afr.

Compaire, J.C., Irigoyen, A.J., Simionato, C.G., Acha, E.M., 2026. Multiscale environmental forcing of multispecies fishery dynamics across climate timescales. Fish. Oce. 1–23. https://doi.org/10.1111/fog.7006.

Compaire, J.C., Visintini, N., Soriguer, M., Johnson, M., Hull, S., Barrett, C., 2024. *Lipophrys pholis* is larger, grows faster and is in better condition in protected than in unprotected rocky shores. Aquat. Conserv. Mar. Freshw. Ecosyst. 34, e4083. https://doi.org/10.1002/aqc.4083.

CTMFM, 2025. Gestión de los recursos pesqueros compartidos 2023-2024. Estado de los recursos pesqueros administrados por la CTMFM en el área. Del. Tratado Del. R. ío De. la Plata Y. su Frente Mar. ítimo 190.

De Wysiecki, A., Milessi, A., Wiff, R., Jaureguizar, A., 2018. Highest catch of the vulnerable broadnose sevengill shark *Notorynchus cepedianus* in the south-west Atlantic (URL). J. Fish. Biol. 92, 543–548. https://doi.org/10.1111/jfb.13532. https://onlinelibrary.wiley.com/doi/10.1111/jfb.13532 (URL).

De Wysiecki, A., Sánchez-Carnero, N., Irigoyen, A., Milessi, A., Colonello, J., Bovcon, N., Cortés, F., Barbini, S., Cedrola, P., Coller, N., Jaureguizar, A., 2020. Using temporally explicit habitat suitability models to infer the migratory pattern of a large mobile shark. Can. J. Fish. Aquat. Sci. 77, 1529–1539. https://doi.org/10.1139/cjfas-2020-0036.

Dulvy, N., Pacoureau, N., Matsushiba, J., Yan, H., VanderWright, W., Rigby, C., Finucci, B., Sherman, C., Jabado, R., Carlson, J., Pollom, R., Charvet, P., Pollock, C., Hilton-Taylor, C., Simpfendorfer, C., 2024. Ecological erosion and expanding extinction risk of sharks and rays. Science 386 (80). https://doi.org/10.1126/science.adn1477.

Engelbrecht, T., Kock, A., O'Riain, M., Mann, B., Dunlop, S., Barnett, A., 2020. Movements and growth rates of the broadnose sevengill shark *Notorynchus cepedianus* in southern Africa: results from a long-term cooperative tagging programme. Afr. J. Mar. Sci. 42, 347–359. https://doi.org/10.2989/1814232X.2020.1802776.

Erzini, K., 1994. An empirical study of variability in length-at-age of marine fishes. J. Appl. Ichthyol. 10, 17–41. https://doi.org/10.1111/j.1439-0426.1994.tb00140.x.

Fabens, A., 1965. Prop. fitting Von. Bertalanffy Growth curve.

Finucci, B., Barnett, A., Cheok, J., Cotton, C., Kulka, D., Neat, F., Pacoureau, N., Rigby, C., Tanaka, S., Walker, T. (2020). Notorynchus cepedianus. The IUCN Red List of Threatened Species 2020: e.T39324A2896914. doi:10.2305/IUCN.UK.2020-3.RLTS.T39324A2896914.en.

Foro para la Conservación del Mar Patagónico y Áreas de Influencia (2008). Estado de conservación del Mar Patagónico y áreas de influencia. Edición del Foro, Puerto Madryn, Argentina.

Francis, M.P., Campana, S.E., Jones, C.M., 2007. Age under-estimation in New Zealand porbeagle sharks (*Lamna nasus*): is there an upper limit to ages that can be determined from shark vertebrae? Mar. Freshw. Res. 58 (1), 10–23. https://doi.org/10.1071/MF06069.

Francis, R., 1988. Maximum likelihood estimation of growth and growth variability from tagging data. New. Zeal. J. Mar. Freshw. Res. 22, 43–51. https://doi.org/10.1080/00288330.1988.9516276.

Frisk, M.G., Miller, T.J., Fogarty, M.J., 2001. Estimation and analysis of biological parameters in elasmobranch fishes: a comparative life history study. Can. J. Fish. Aquat. Sci 58 (5), 969–981. https://doi.org/10.1139/f01-051.

Funes, M., De Wysiecki, A., Bovcon, N., Jaureguizar, A., Irigoyen, A., 2024. Understanding the feeding ecology of the broadnose sevengill shark (*Notorynchus cepedianus*) in Patagonia, Argentina. Food Webs 38, e00339. https://doi.org/10.1016/j.fooweb.2024.e00339.

García-García, D., Cousido-Rocha, M., Bañón, R., Campelos, J.M., Quintero, F., Gancedo, A., Lamas, F., Otero, A., Rodríguez, A., Alonso-Fernández, A., 2026. Length-based stock assessment in small-scale multi-gear fisheries: insights from a European hotspot (NW Spain). Rev. Fish Biol. Fish. 36 (1), 31. https://doi.org/10.1007/s11160-026-10036-5.

Goldman, K.J., Cailliet, G.M., Andrews, A.H., Natanson, L.J., 2012. Assessing the age and growth of chondrichthyan fishes. Biol. Sharks their Relat. 13, 423.

Gompertz, B., 1825. On the nature of the function expressive of the law of human mortality, and on a new mode of determining the value of life contingencies. Philos. Trans. R. Soc. Lond. 513–583. https://doi.org/10.1098/rstl.1825.0026.

Guzmán, M., Campodónico, G., 1976. *Notorynchus cepedianus* (Peron, 1807) en la entrada oriental del Estrecho de Magallanes (Elasmobranchii, Hexanchidae). An. Del. Inst. la Patagon. 7, 207–210.

Harry, A.V., 2018. Evidence for systemic age underestimation in shark and ray ageing studies. Fish Fish. 19 (2), 185–200. https://doi.org/10.1111/faf.12243.

Harry, A.V., Smart, J.J., Pardo, S.A., 2022. Understanding the age and growth of Chondrichthyan fishes. Biol. Sharks Their Relat. 177–202.

Irigoyen, A., Bovcon, N., Trobbiani, G., De Wysiecki, A., Argemi, F., Jaureguizar, A.J., 2019. Habitat use, seasonality and demography of the broadnose sevengill shark *Notorynchus cepedianus* in central Patagonia: Another piece of the puzzle. Austral Ecol. 44, 1463–1470. https://doi.org/10.1111/aec.12820.

Irigoyen, A., De Wysiecki, A., Trobbiani, G., Bovcon, N., Awruch, C., Argemi, F., Jaureguizar, A., 2018. Habitat use, seasonality and demography of an apex predator: sevengill shark *Notorynchus cepedianus* in northern Patagonia. Mar. Ecol. Prog. Ser. 603, 147–160. https://doi.org/10.3354/meps12715.

Irigoyen, A., Sibbald, C., Cuestas, M., Cristiani, F., Trobbiani, G., 2015. Patrones estacionales de abundancia en el Golfo Nuevo y migración a lo largo de la plataforma Argentina de cazones (*Galeorhinus galeus* [Linnaeus 1758]) y gatopardos (*Notorynchus cepedianus* [Péron 1807]) (Argentina). Ecol. Austral 25, 144–148.

Irigoyen, A., Trobbiani, G., 2016. Depletion of trophy large-sized sharks populations of the Argentinean coast, south-western Atlantic: insights from fishers' knowledge. Neotrop. Ichthyol. 14. https://doi.org/10.1590/1982-0224-20150081.

Jaureguizar, A., Cortés, F., Braccini, J., Wiff, R., Milessi, A., 2022. Growth estimates of young-of-the-year broadnose sevengill shark, *Notorynchus cepedianus*, a top predator with poorly calcified vertebrae. J. Fish. Biol. 100, 625–631. https://doi.org/10.1111/jfb.14976.

Jaureguizar, A., De Wysiecki, A., Cortés, F., Milessi, A., 2023. An estuarine system as a possible nursery habitat for the broadnose sevengill shark: San Antonio cape—Southwest Atlantic. Hydrobiologia 850, 4149–4169. https://doi.org/10.1007/s10750-023-05293-5.

Katsanevakis, S., Maravelias, C., 2008. Modelling fish growth: multi-model inference as a better alternative to a priori using von Bertalanffy equation. Fish Fish. 9, 178–187. https://doi.org/10.1111/j.1467-2979.2008.00279.x.

Last, P., Stevens, J., 1994. Sharks and rays of Australia.

Liu, K., Wu, C., Joung, S., Tsai, W., Su, K., 2021. Multi-Model Approach on Growth Estimation and Association With Life History Trait for Elasmobranchs. Front. Mar. Sci. 8, 1–13. https://doi.org/10.3389/fmars.2021.591692.

Lucifora, L., Menni, R., Escalante, A., 2005. Reproduction, abundance and feeding habits of the broadnose sevengill shark *Notorynchus cepedianus* in north Patagonia, Argentina. Mar. Ecol. Prog. Ser. 289, 237–244. https://doi.org/10.3354/meps289237.

Mace, G., Collar, N., Gaston, K., Hilton-Taylor, C., Akçakaya, H., Leader-Williams, N., Milner-Gulland, E., Stuart, S., 2008. Quantification of Extinction Risk: IUCN's System for Classifying Threatened Species. Conserv. Biol. 22, 1424–1442. https://doi.org/10.1111/j.1523-1739.

Marcovecchio, J.E., De Marco, S.G., Gavio, M.A., Narvarte, M., Fiori, S., Gerpe, M.S., Botté, S.E., 2019. The northern Argentine sea. World Seas: An Environmental Evaluation. Academic Press, pp. 759–781.

McFarlane, G.A., King, J.R., Saunders, M.W., 2002. Preliminary study on the use of neural arches in the age determination of bluntnose sixgill sharks (*Hexanchus griseus*). Fish. Bull. 100 (4), 861–864.

Milessi, A. (2008). Modelación ecotrófica en el ecosistema costero bonaerense (34°-41°S) años 1981-83. Technical Report. INIDEP. Mar del Plata, Argentina.

Natanson, L.J., Skomal, G.B., Hoffmann, S.L., Porter, M.E., Goldman, K.J., Serra, D., 2018. Age and growth of sharks: do vertebral band pairs record age? Mar. Freshw. Res. 69 (9), 1440–1452. https://doi.org/10.1071/MF17279.

Passerotti, M.S., Andrews, A.H., Carlson, J.K., Wintner, S.P., Goldman, K.J., Natanson, L. J., 2014. Maximum age and missing time in the vertebrae of sand tiger shark (*Carcharias taurus*): validated lifespan from bomb radiocarbon dating in the western North Atlantic and southwestern Indian Oceans. Mar. Freshw. Res. 65 (8), 674–687. https://doi.org/10.1071/MF13214.

Pauly, D., 1980. On the interrelationships between natural mortality, growth parameters, and mean environmental temperature in 175 fish stocks. ICES J. Mar. Sci. 39, 175–192. https://doi.org/10.1093/icesjms/39.2.175.

Pauly, D., 1984. Fish population dynamics in tropical waters: a manual for use with programmable calculators, 8. WorldFish.

Petetta, A., Li Veli, D., La Mesa, M., Grati, F., Bolognini, L., 2025. Catch, release and second chances: exploring the impact of angling on two coastal fish species. Front. Mar. Sci. 12, 1638216. https://doi.org/10.3389/fmars.2025.1638216.

Pilling, G., Cotter, A., Metcalfe, J. (2007). Data for Assessment and Research. Technical Report.

Riverón, S., Raoult, V., Slip, D.J., Mas, F., Laporta, M., Pereyra, I., Harcourt, R.G., 2025. Shearing Tooth Morphology May Allow Sharks to Access Higher Trophic Levels at Smaller Sizes. Ecol. Evol. 15 (8), e71722. https://doi.org/10.1002/ece3.71722.

Robertson, T.B., 1923. Chem. Basis Growth Senescence.

Sadowsky, V., 1969. First record of broad-snouted seven-gilled shark from Cananéia, coast of Brazil. Bol. do Inst. Ocean. 18, 33–35.

Seabold, S., Perktold, J., 2010. Statsmodels: econometric and statistical modeling with python. 9th Python Sci. Conf. 92–96.

Silveira, S., Laporta, M., Pereyra, I., Mas, F., Doño, F., Santana, O., 2018. Análisis de la captura de condrictios en la pesca artesanal oceánica de Uruguay. Atl. ántico Sudoccidental. Frente Mar. ítimo 25, 301–324.
Simpfendorfer, C., 2000. Growth rates of juvenile dusky sharks, *Carcharhinus obscurus* (Lesueur, 1818), from southwestern Australia estimated from tag-recapture data. Fish. Bull. 98, 811–822.
Taylor, C.C., 1958. Cod growth and temperature. J. Cons. Cons. Int. Fxplor. Mer. 23, 366–370.
Terpilowski, M., 2019. scikit-posthocs: Pairwise multiple comparison tests in Python. J. Open. Source Softw. 4, 1169.
Van Dykhuizen, G., Mollet, H., 1992. Growth, age estimation and feeding of captive Sevengill Sharks, *Notorynchus cepedianus*, at the Monterey Bay Aquarium. Aust. J. Mar. Freshw. Res. 43, 297–318. https://doi.org/10.1071/MF9920297.
Virtanen, P., Gommers, R., Oliphant, T., Haberland, M., Reddy, T., Cournapeau, D., Vázquez-Baeza, Y., 2020. SciPy 1.0: fundamental algorithms for scientific computing in Python. Nat. Methods 17, 261–272. https://doi.org/10.1038/s41592-019-0686-2.
Wells, D.R.J., Smith, S.E., Kohin, S., Freund, E., Spear, N., Ramon, D.A., 2013. Age validation of juvenile shortfin mako (*Isurus oxyrinchus*) tagged and marked with oxytetracycline off southern California. Fish. Bull. 111 (2).